25

Colloidal Crystals

E. C. H. Ng[1], Y. K. Koh[2] and C. C. Wong[1]
[1]*Singapore-MIT Alliance, Nanyang Technological University,*
[2]*DSO National Laboratories,*
Singapore

1. Introduction

A colloidal system consists of insoluble particles well-dispersed in a continuous solvent phase, with dimensions (generally less than 1μm in at least one important dimension) that are relatively larger than the molecules of the solvent. When the particles in this system are arranged in periodic arrays, analogous to a standard atomic crystal with repeating subunits of atoms or molecules, they form colloidal crystals (Pieranski, 1983). Gem opal (silica particles in close packed arrangement), iridescent butterfly wings made of periodic and spongelike pepper-pot structure (Biró et al, 2003) and sea mouse with hexagonal close packed structure of holes (McPhedran et al, 2003) are typical examples of colloidal crystals found in nature.

In 1935, discovery of tobacco and tomato virus by Stanley (Kay, 1986) provided excellent examples of naturally occurring monodisperse colloidal crystals. By centrifuging the dilute suspension of virus particles, crystals formed at the bottom of centrifuge tube can be examined by X-ray or light diffraction. The ease to obtain close-packed arrangement of colloidal particles has fascinated many, especially researchers working in chemical sensors, photonic band gap (PBG[1]) crystals, nanopatterning and sensors. 3D Colloidal crystals with periodicity ranging from 100nm to 1μm diffract visible wavelength according to Bragg's law, serving as waveguide and reflective surfaces for many useful devices in communication (Avrutsky et al, 2000; Liu, 2005) and solar harvesting (Mihi et al, 2011). Monolayers of colloidal arrays can serve as lithography mask (Lee et al, 2010) and physical mask for nanoimprinting. Periodicity can then be manipulated with the right particle size.

In this chapter, we discuss briefly the concepts of a colloidal system and types of interaction that give rise to crystallization, growth techniques and characterization tools available to help readers who are interested and new to colloidal systems. However, we limit the scope to simple colloidal particles which are spherical and of identical size, despite the possibility to self-assemble colloidal structures of complicated dimensions (Chen et al, 2006; Lu et al, 2001). Of the many growth methods, we place particular emphasis on capillary growth and its dependence on interparticle interactions, the substrate, and the manipulation of the solvent meniscus.

[1]Photonic band gap crystals are periodic structures which are able to block light propagation through the crystal in one or more directions. (Yablonovitch, 1987)

2. General concepts of a colloidal system

2.1 Colloidal system as a model for condensed matter

Colloidal systems share several similar cooperative phenomena with condensed matter (atomic crystal): ordering, phase transitions and stability of the resulting phases. As the ratio of colloidal particle size to atomic dimension is huge (~10^3), parameters like the time scales of diffusion and lattice distances are also scaled up appropriately to milliseconds and micrometers respectively. This allows one to probe into real time processes that are otherwise inaccessible in atomic systems (Arora & Tata, 1996). As a result, a suspension of colloidal particles has provided fascinating models to investigate the physics of nucleation and growth (Gasser et al, 2001; Habdas & Weeks, 2002), phase transitions (Bartlett et al, 1992; Gast & Russel, 1998; Sirota et al, 1989), and fundamental problems of crystallization kinetics (Auer & Frenkel, 2001; Yethiraj et al, 2004).

A stable suspension of monodisperse colloidal particles normally appears milky white and will only become iridescent when interparticle distance shrinks to submicron range and satisfy Bragg's diffraction. Extensive study of equilibrium phase behavior of monodisperse colloidal system has shown that face-centered cubic (fcc) ordering is the equilibrium phase (Hales, 1997), above a threshold volume fraction (Pusey & Megan, 1986). Interestingly, body centered cubic (bcc) system was also discovered at ionic strength lower than 2.7 x 10^{-6} M KCl and volume fraction less than 0.008 (Monovoukas & Yiannis, 1989). The ability to change interparticle forces using electrolytes soon becomes a major advantage of colloidal system in modeling condensed matter.

Understanding all the interaction forces involved for particles in close proximity is nontrivial, as their magnitude or strength will decide their stability in suspension (no aggregation), ease of crystallization and final packing arrangement. Since many practical applications in interface science and colloidal science revolve around the problems of controlling forces between colloidal particles and between surfaces of different curvatures, many have devoted considerable effort to model surface forces and engineer their interactions in either short range or long range. It is impossible to give a detail perspective for all proposed models regarding colloids, only a few important concepts are introduced here, chosen based on the authors' preference for convenience. A more comprehensive review of all the interactions involved can be found in "Ordering and Phase transitions in Charged Colloids" (Arora & Tata, 1996).

2.2 Hard sphere model

One can first treat colloidal particles as hard and electrically neutral particles. Besides van der Waals forces, they only interact by steric repulsion when they are brought into physical contact. For monodisperse spherical particles, the close-packing limit is 0.74, which is equivalent to atomic packing factor of fcc atomic crystal. In another words, fcc packing arrangement would be the most stable form of colloidal crystal at equilibrium.

In practice, high concentration of colloidal suspension tends to flocculate before maximum packing limit is reached. Brownian motion allows particles to gain thermal energy easily and collide with each other to form clusters. If many aggregates form upon collision (especially at high temperature and high concentration), there is a high chance that amorphous colloidal aggregates will form, preventing further packing. In order to obtain FCC crystal structure, slow sedimentation of large particles in less concentrated suspension (volume fraction, v.f. << 0.5) by gravitational forces was explored (Crandall & Williams,

1977; Mayoral et al, 1997; Míguez et al, 1997). A phase transition from fluid to crystal can be observed as the local volume fraction increases beyond 0.49 (Pussey & Megan, 1986). This process is rather slow and may take up to a few days to weeks, depending on the initial concentration and desired volume of crystal grown.

In 1968, Hoover and Francis confirmed the existence of first-order melting transition for colloidal hard spheres and reported the densities of coexisting phases via Monte Carlo simulation (Hoover & Ree, 1968). It was found that melting and crystallization occur at reduced pressure of p = 8.27. The corresponding volume fractions, Φ is thus in the range of 0.50 to 0.55.

2.3 Charged spheres

Almost all colloidal particles are not electrically neutral. They may contain a large number of acid, base or other functional groups which are susceptible to dissociation in a polar solvent. Their functional groups are normally determined by the synthesis path or catalysts used. For instance, polystyrene beads synthesized using KPS (Potassium persulfate) catalyst will give rise to negatively charged particles. Hence, hard sphere model using exclusively steric repulsion is only a good approximation, but not an accurate approach to address real colloidal system.

Fig. 1 depicts the charge distribution surrounding negatively charged particles in water suspension. Given a neutral system of suspension, each colloidal particle of radius R carries negative charges of Ze. The water solvent contains an equivalent amount of counterions as well as possible stray ions such as salt (Na^+ and Cl^-). In a pure colloidal suspension with no salt present, the negative charges on particle surfaces will form thick double layer (~10^1 nm) and exert repulsion on each other, preventing formation of particle clusters. Part of the counterions will be attracted to near surface of negatively charged particles, while the remaining can move around in bulk suspension. If a small amount of salt (e.g. NaCl) is added into the colloidal system, positive ions (Na^+) will be attracted to particle surface, screening the repulsions between negatively charged particles. As a result, interparticle distance decreases and the attraction between particles could be enhanced. Super high salt concentration will collapse the double layer, and if the particles happen to be in physical contact by chance (Brownian motion), they will form irreversible aggregates immediately, giving no chance of forming ordered structures.

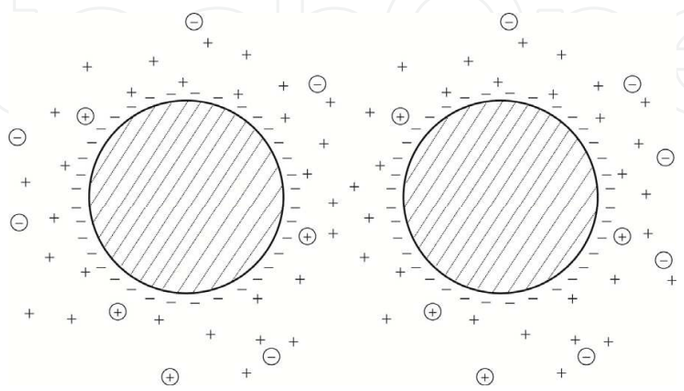

Fig. 1. Colloidal particles of radius R carrying negative charge -, with counterions + present in vicinity. + and – signs which are enclosed in circles represent stray ions.

2.4 DLVO model

To further assist reader, a model based on DLVO theory is introduced. It is named after Derjaquin, Landau, Verwey and Overbeek. The theory describes the interaction forces between charged surfaces in a liquid medium. It combines both the van der Waals forces and electrostatic interaction of charged surface, computed in mean field approximation in the limit of low surface potentials.

Here, it is assumed that:

a. Each colloidal particle is surrounded by its own double layer and behaves as if it was electrically neutral unless it approaches another particle closely enough
b. Only small and very mobile ions are first allowed to move. The mean field must be consistent with the boundary conditions on the surface of colloidal particles in suspension and the distribution obeys Boltzmann statistics (Brownian motion).
c. The potential energy of an elementary charge on a surface is much smaller than the thermal energy, kBT.
d. The particles are allowed to change position and find their own equilibrium states.

For DLVO potential,

$$V_{DLVO} = \frac{64\pi R c_o \Gamma_o^2 kT}{k^2} \exp(-\kappa r) - \frac{AR}{12r} \tag{1}$$

R is particle radius, c_o is ion concentration, k is Boltzmann constant, T is temperature, κ is inverse double layer thickness, r is separation between particles, and A is Hamaker constant. Surface potential of particles can be described by

$$\Gamma_o = \tanh\left(\frac{ze\Phi_o}{4kT}\right) \tag{2}$$

where z is valence of counter ions, e is the electronic charge, and Φ is the surface potential.

It is obvious that the first part of equation (1) is related to electric double layer interaction (repulsion by similar charge of particles) where as the second part can be referred to attractive van der Waals interaction. As discussed earlier, electric double layer provides an energy barrier against irreversible agglomeration. This energy barrier, as indicated in Fig. 2 (right) as V_{max}, normally has a magnitude ranging from 0 ~ 100 kT, depending on the suspension parameters. Unlike the atomic model, two minima exist between two approaching colloidal particles, which are irreversible (primary) and reversible (secondary) respectively. In atomic crystals, atoms are held strongly in the single equilibrium position (as indicated in Fig. 2 (left)). High energy barrier or chemical bonds must be broken to disrupt the ordering. A brief comparison of interaction potential between atoms and colloidal particles in close proximity is best illustrated in Fig. 2 for clarity.

Surprisingly, the existence of secondary minimum allows scientists to "anneal" or remove defects in ordered arrays of wet colloidal crystal at this metastable state, before reaching the final irreversible dry state of colloidal crystal. The related works of particulate mobility in wet colloidal crystal will be further discussed in section 3.2.

For crystallization to occur, van der Waals forces must exceed double layer repulsion. This could only happen when particles are so close enough, overcoming the energy barrier V_{max}. This is possible as double-layer interaction energy is finite or increases slowly when r approaches zero, while V_{vdw} decreases exponentially when $r \rightarrow 0$. Unlike electrostatic

interaction, van der Waals interaction is highly insensitive to the change of pH and electrolyte concentration. Small addition of salt may change the magnitude of V_{max} significantly and remove the secondary minimum. Thus, no ordering in long range is ever possible if this situation happens.

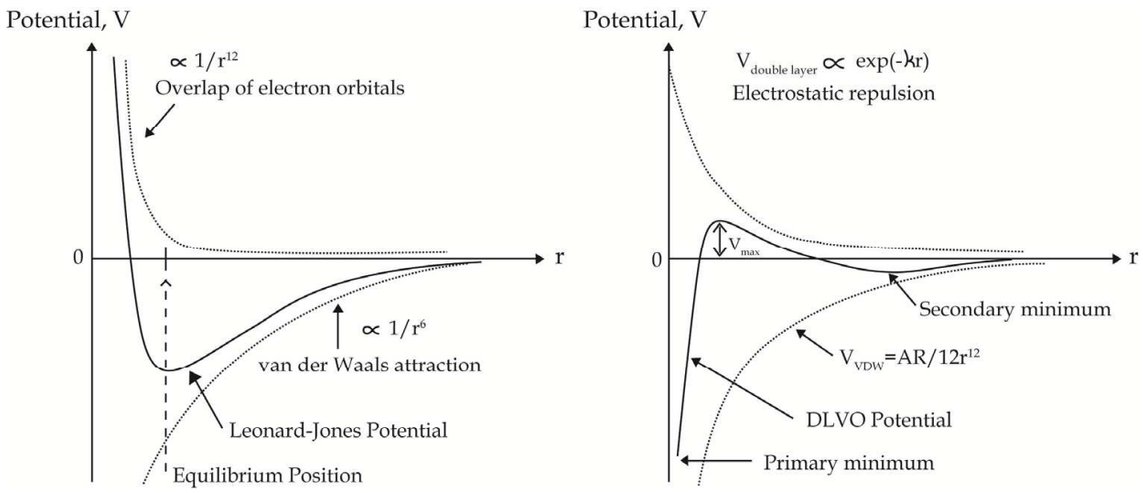

Fig. 2. A comparison of interaction potentials between atoms (Left) and colloidal particles (Right) in close proximity, described by Leonard-Jones potential and DLVO potential respectively.

3. Ordering and kinetics of colloidal particles

The ordering and kinetics of colloidal particles could be quite different from atomic crystals. The medium of colloidal dispersion gives rise to the dynamic motion of particles (Brownian) and exerts capillary forces on the particles near the interfaces (Kralchevsky & Nagayama, 1994). Fluid instability at interface (e.g. dewetting) further complicates the kinetics of crystallization process (Davis, 1980; Troian, 1989). All these contribute to several technical issues in achieving perfect crystal growth.

Hence, it is important to address the relevant critical forces involved in particle ordering. First, the proposed mechanism will be presented here with supporting research works from literature review and authors' publications. However, the discussion will be mostly focused on assembly process induced by capillary forces. Other assembly methods like e-field induced assembly (Holgado et al, 1999; Prieve et al, 2010; Yethiraj and Blaaderen, 2003; Zhang & Liu, 2004) and spin-coating assembly (Jiang & McFarland, 2004) can be referred to the recommendations in the reference list.

As mentioned in section 2, self-assembly via gravitation force is rather slow, and limits its application. Besides, the particles will only settle if their size and density is sufficiently high. This sedimentation tendency is best characterized by the Peclet number (see equation 3). Hence, this practical issue led to the studies of filtration and centrifugation (Park et al, 1999; Velev & Lenhoff, 2000), which however do not necessarily offer good control over packing quality and thickness of crystal grown. The formation of polycrystalline domains with different lattice orientation in colloidal crystals is commonly found, possibly due to nucleation at different locations of the specimen surface and the subsequent growth of crystal domains in different directions (Pusey et al, 1989).

Here we describe colloidal self-assembly under the effect of evaporation and capillary force, a phenomenon observed in the "coffee-ring" experiment [Deegan et al, 1997]. When a drop of coffee is spilled onto a solid substrate, a dense ring of stain will be formed upon drying, leaving the center of the initial droplet empty. The dense deposition of coffee solids near the outer ring signifies an intense movement of solid particles from the droplet interior to the drying perimeter. This driving force is attributed to evaporation, causing outward capillary flow (both solvent and solids) to the pinned contact line of the drying droplet, in order to replenish solvent loss from the edge (Dushkin et al, 1993). Deegan and his group then confirmed a power-law growth of ring mass with time in coffee-ring deposition, a mechanism which is independent of substrate type, carrier fluid and deposited solids. In short, the deposition process could be very fast, depending only significantly on the evaporation rate.

Dating back to 1992, the mechanism and stages of evaporation-induced assembly was first investigated in detail using an experimental cell containing a thin well of monodisperse micrometer-size latex particles, which allowed in-situ microscopic observation (Denkov et al, 1992). Similar to coffee-ring experiment, the particles were brought convectively to the edge of evaporation front, and the ordering of particles was found to be initiated when the thickness of water layer approached the underlying diameter of particles. Examples of particles moving to the drying edge of water film are shown in Fig. 3 and Fig. 4. Self-assembly starts when water thickness is about one particle diameter (860 nm) and it is normally monolayer near the perimeter of drying droplet.

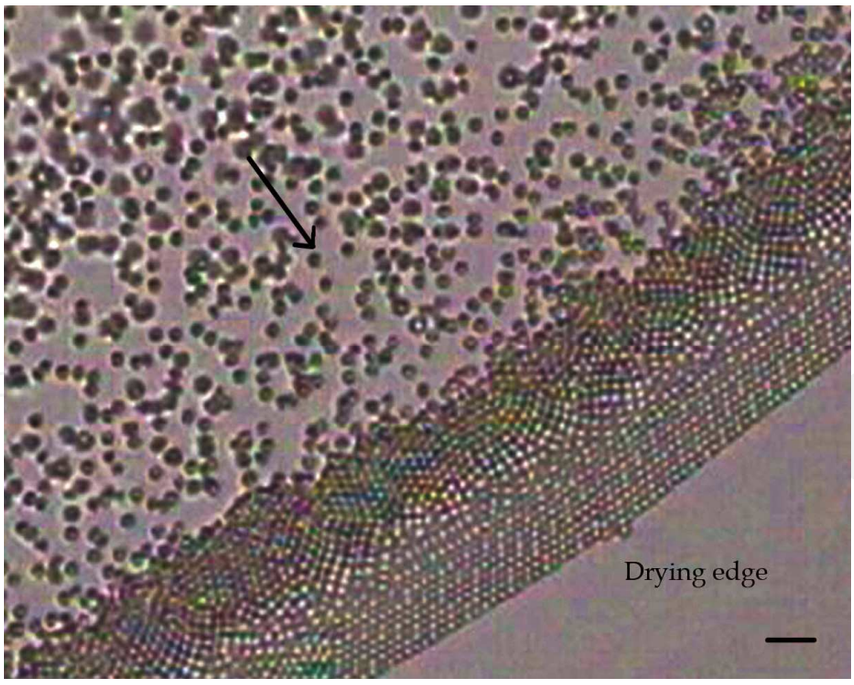

Fig. 3. Evaporation driven self-assembly in sessile droplet. Polystyrene particles (860 nm) move convectively to the drying edge, forming monolayer crystal at the outer perimeter. Transitional phases (e.g. buckling, square) are observed few particle diameters away from the perimeter (copyright reserved). Arrow indicates the direction of particle movement.

In evaporation-induced self-assembly, much attention is paid to the drying stage when the thickness of water layer is close to particle diameter. As evaporation proceeds, thinning of water layer causes deformation of menisci (shown in Fig. 4) between particles at drying front. Further evaporation from the concave menisci increases the curvature and local capillary pressure, driving more water influx from thicker water layer to thinner region. Partially immersed particles also experience capillary attraction, leading to further packing of particles to form close-packed crystal. It is also worth noting that large and partially submerged particles can be immobilized by the thinning water layer as the vertical component of surface tension force pressing the particles against the horizontal substrate is huge. This phenomenon also serves as a condition for contact line pinning, which we will discuss later in section 4.2. Besides, formation of multilayer colloidal crystal is possible if wetting angle is large or thickness of water layer is large (Jiang et al, 1999).

Due to the almost fixed contact line formed by colloidal droplet on horizontal substrate, a variation of colloidal crystal thickness is commonly observed, from one single layer near the edge to multilayer further away from the contact line (Fig. 3). In spite of evaporation, slight reduction of water layer thickness over time does not help in the uniformity. Hence, an approach to let contact line move along deposition direction was introduced. Fig. 5 illustrates an experimental setup of vertical deposition, where a substrate is submerged vertically or at an inclined angle inside a colloidal suspension of dilute concentration (< 0.1 volume fraction). The temperature of the suspension can be controlled by a water bath surrounding the suspension, driving the convective flow of particles to contact line for controlled deposition. As long periods of evaporation may change suspension concentration over time, the temperature is normally adjusted to be very low, close to room temperature. Then the moving contact line is driven accordingly by withdrawing the substrate or pumping out the colloidal suspension at a controlled speed (Zhou & Zhao, 2004). The speed of the moving contact line will then determine the thickness of colloidal crystal obtained.

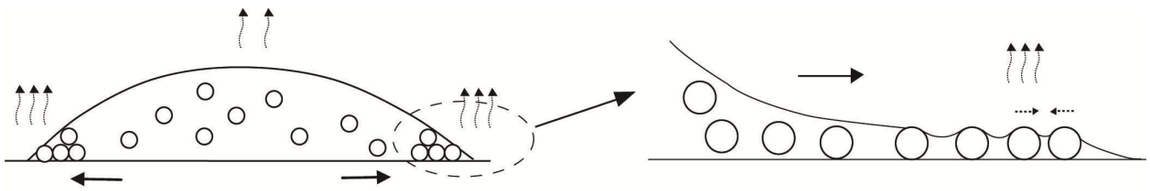

Fig. 4. Sessile droplet of colloidal suspension is shown on the left and a magnified version of thinning water layer of colloidal particles is depicted on the right. The scaling is for illustration purpose only. Curvy arrows indicate evaporation or water loss, which is faster at the edge. Straight arrows indicate convective flow of particles to the edge of sessile droplet. And dashed arrows on the right figure indicate capillary attraction between two partially submerged particles.

Other parameters such as incline angle of submerging substrate, surfactant addition, evaporation rate, ambient temperature, solvent volatility, particle concentration and substrate hydrophilicity have been explored to control the thickness of deposition (Denkov et al, 1992; Dimitrov & Nagayama, 1996; Im et al, 2003; Jiang et al, 1999; Kralchevsky & Denkov, 2001; Mclachlan, 2004). All these parameters must be optimized together with the speed of moving contact line, in order to obtain large area of uniform colloidal crystal.

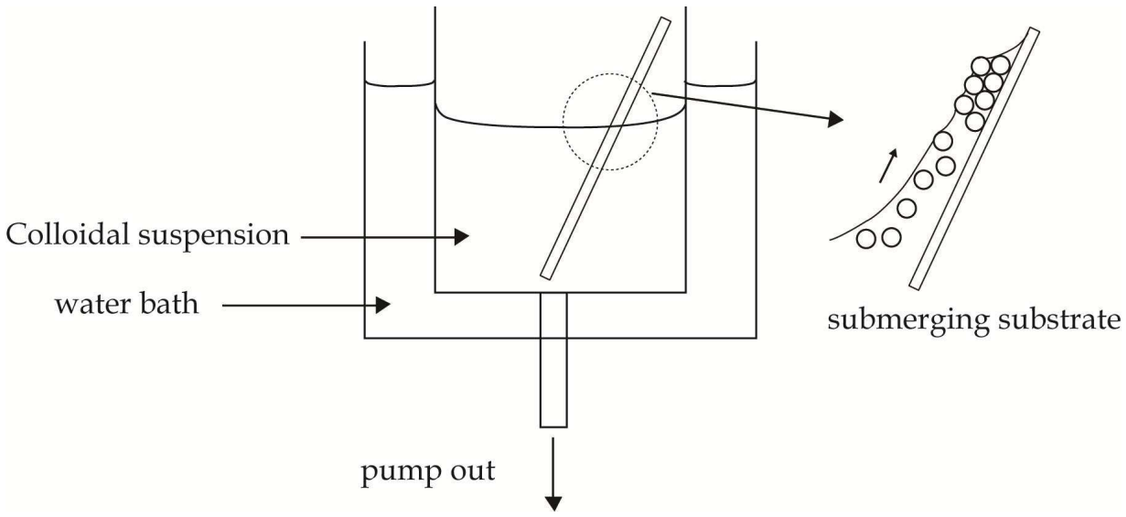

Fig. 5. Figure depicts an experimental setup for flow-controlled vertical deposition, an assembly method to control movement of contact line along crystal growth direction (Zhou & Zhao, 2004). Inset on the right shows capillary rise region near the submerged substrate.

3.1 Kinetic stages of colloidal crystallization

Since capillary forces can be significant in influencing the final assembly during drying process, systems with continuous environmental changes must be taken into account if one aims to design a process to obtain long-range ordered structures. There was also a desire to correlate the microscopic interaction and macroscopic boundary forces to provide a more complete model of colloidal self-assembly. The macroscopic forces are primarily capillary forces experienced by partially immersed particles under the thinning of water layer. The microscopic forces are contributed by electrostatic, steric interactions and van der Waals forces between closely arranged particles. In the case of larger particles, they will experience stronger effect of macroscopic boundaries before they have a chance to interact by microscopic forces. One can assume dominant function of capillary forces in this type of system. On the contrary, particles which are relatively smaller than the volume in which they are confined will be driven by microscopic interaction forces before experiencing capillary forces.

In order to understand the transition dynamics from well-dispersed colloids in suspension to dry colloidal crystalline film by evaporation-induced self-assembly, in situ transmission spectroscopy was introduced to monitor the assembly stages (Koh & Wong, 2006; Koh et al, 2008). Treating the assembly process as an emergent photonic crystal, several sequential stages of colloidal ordering with different lattice parameters in wet suspension could be interpreted based on Bragg's law (equation 4). Fig. 6 depicts an experimental setup by Koh et al, to investigate the self-assembly stages at the meniscus near the contact line formed on vertical substrate in vertical deposition.

Due to the good wettability of the hydrophilic glass substrate, thin meniscus formed near the substrate was higher than the bulk meniscus, providing a clear line of sight for transmitted beam. As evaporation proceeds, consistent arrival flux of particles at the thin meniscus could either stay or sediment back into bulk suspension. The tendency to sediment can be described by Peclet number, Pe:

$$Pe = m_B g R / kT \tag{3}$$

where m_B is buoyancy mass of a particle with radius R and g is the gravitational acceleration. This number is also a good indicator to determine the stability of a colloid suspension. For Pe >> 1, the particles will tend to sediment and form agglomerates. In vertical deposition, commonly used particles are small, having Pe of unity or smaller. For instance, polystyrene spheres of 0.1 μm and 10 μm in water solvent at a temperature of 23°C give Peclet number of 5×10^{-5} and 5030 respectively.

A sequence of transmission spectra were taken from time t_1 to t_5, as shown in Fig. 7. The diffraction features shown in Fig. 7 can be correlated to photonic band gap structures (Ho et al, 1990; Koh et al, 2008). Under slow evaporation, it can be assumed that ordering in the suspension will lead to the equilibrium FCC structure (Monovoukas & Yiannis, 1989). Besides, (111) plane of colloidal crystal obtained is confirmed to be parallel to the substrate, providing an important reference for photonic band gap calculation

The spectra was at first featureless as light was hardly transmitted due to random scattering by the disordered structure. As local volume fraction at thin meniscus increases with evaporation, first feature A was observed at t_1 (300 min). This indicates the onset of order in the colloidal suspension: the first kinetic stage of ordering. Here, the rising local concentration shrinks the average distance between particles. Since particles are fully submerged in solvent, it is believed that the interaction forces between the particles are the only driving force for ordering, overwhelming the randomizing Brownian forces. It is also found that feature A corresponds to a larger lattice parameter (368nm) of fcc colloidal crystal, compared to 276 nm of the expected equilibrium colloidal crystal formed by hard-sphere packing of the polystyrene particles with diameter of 195 nm. This transition structure is stabilized by the interparticle forces, in which the existence of DLVO potential barriers prevents the particles from coming into direct contact. Here, we treat the interaction potential between two particles in a solvent using DLVO theory (see section 2.4) where the total potential is taken as the sum of the repulsive and attractive forces.

With continued growth of the colloidal crystal, a second feature (B) appears at a shorter wavelength (from t_2 onwards in Fig. 7). This corresponds to wet FCC colloidal crystal with the particles in direct physical contact (zero separation) with water in the interstices. Water-retaining capillary pores are normally formed in the interstices of deposited colloidal crystal as the meniscus recedes below the self-ordered crystal. The subsequent loss of water upon drying of wet colloidal crystal immediately gives rise to a blue shift, feature C at t_4 (770 min) and t_5 (800 min), which can be correlated to the change of dielectric contrast as water in the interstices is replaced by air. In the transitions from t_1 to t_3 and t_3 to t_5, coexistences of the two features A and B are observed at t_2 and t_4 simultaneously. These are likely due to the simultaneous existence of the corresponding transition structures where not all region of wet colloidal crystal shrink and dry at the same time. The growth of intensity for feature B from t_2 to t_3 indicates the area increase of double-layer collapse across the studied area of colloidal crystal (area of the incident light beam). Also, the intensity increase from t_4 to t_5 explains the continual evaporation of water from the wet colloidal crystal to form dry crystal, revealing feature C.

The essence of this work is the demonstration of three distinctive stages in colloidal self-assembly, as shown in Fig. 8. This model is further supported with sequential changes of lattice parameters derived from the transmission spectra in Fig. 7. It was then confirmed that feature A had a lattice parameter of 368 nm, which was larger than the equilibrium colloidal crystal with lattice parameter of 276 nm. The larger interparticle distance in wet suspension during self-assembly indicates the existence of DLVO potential barrier, which prevents

particles from coming into direct contact. This finding highlights the important role of interaction forces for small particles, despite the earlier understanding that colloidal self-assembly at liquid menisci is driven solely by capillary forces. This could only be true for the sizes of the particles that are small relative to the volume that is confined by the macroscopic boundaries. It is believed that the capillary forces are only brought into action from the second stage onwards, where the forces collapse the electric double layer, thus bringing

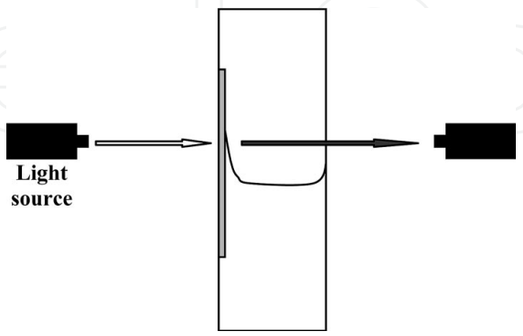

Fig. 6. Schematic shows an in situ transmission spectroscopy of colloidal self-assembly. A glass substrate is located in a plastic cuvette of colloidal suspension. This whole apparatus is kept in a temperature-controlled chamber, which controls evaporation from the suspension. Reprinted with permission from *Langmuir,* Vol. 24, No. 10 (May 2008), pp. 5245-5248. Copyright 2008 American Chemical Society.

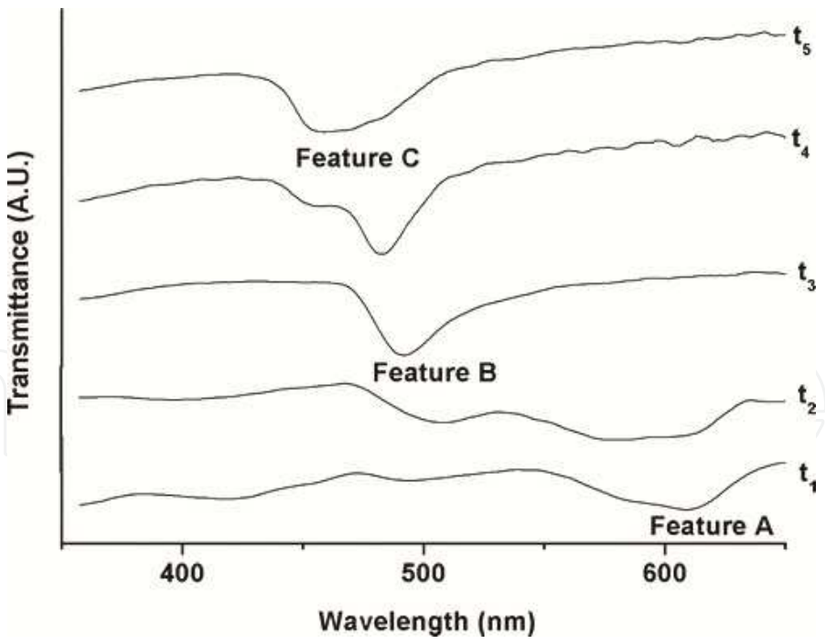

Fig. 7. Transmission spectra show emerging features A (608 nm), B (491 nm), and C (462 nm) at different time interval. Two features are observed simultaneously at times t_2 and t_4. The spectra are offset vertically for clarity. Spectra are taken at t_1 (300 min), t_2 (320 min), t_3 (400 min), t_4 (770 min) and t_5 (800 min). Reprinted with permission from *Langmuir,* Vol. 24, No. 10 (May 2008), pp. 5245-5248. Copyright 2008 American Chemical Society.

particles into direct contact, with solvent trapped in the interstices (Fig. 8, middle). The assembly process then ends with the final replacement of water with air, bringing a change in periodic dielectric contrast as water evaporates from wet colloidal crystal (Fig. 8, Top). Once this stage is achieved, the colloidal crystal obtained will be stable and strong enough to resist structural changes against liquid infiltration process. This robustness enables infiltration with other functional materials to obtain inverse opal structures or opals with different material properties via double templating (Yan et al, 2009).

Understanding the dynamic transition of colloidal crystal may provide some insights towards improving long-range quality of colloidal crystal. First, the electric double layer around each particle must be as thin as possible, and yet prevent premature aggregation. This is because large double layer thickness will give rise to large shrinkage stress during the final collapse of double layer (A to B), resulting in macroscopic cracks (Jiang et al, 1999). In the next section, the manipulation of DLVO potential to study particulate mobility of self-assembly process will be discussed.

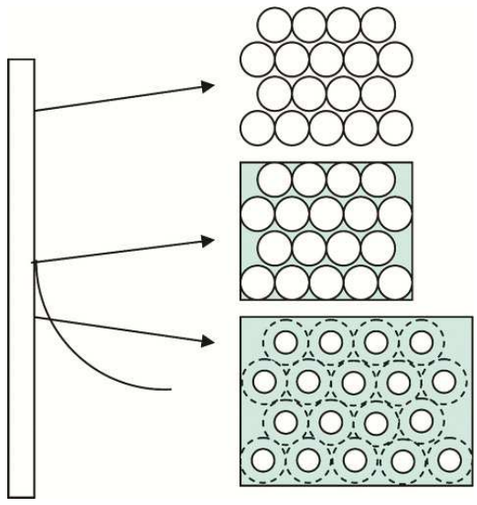

Fig. 8. Three distinct stages in colloidal self-assembly process. First stage (bottom) shows a transition structure with a large lattice parameter, corresponding to feature A in Fig. 7. As the meniscus moves, this structure collapses to a smaller lattice parameter (middle), with water retained in its interstices, giving rise to feature B in the transmission spectra. Finally, a dried colloidal crystal (top) corresponding to feature C is obtained. Reprinted with permission from *Langmuir,* Vol. 24, No. 10 (May 2008), pp. 5245-5248. Copyright 2008 American Chemical Society.

3.2 Particulate mobility in vertical deposition

The absence of repulsion forces between charged particles and oppositely charged surfaces often lead to disordered clustering (Yan et al, 2008). At high particle concentration in a confined volume (e.g. thin meniscus), repulsion force is the key to prevent irreversible clustering and the prerequisite for sufficient particulate mobility to obtain higher packing quality, if sufficient time of ordering is given. Since understanding the collective behavior of the particles in an environment of high mobility is indispensable, the mobility and electrostatic interactions of negatively charged substrates and positive colloids were studied, with optimized parameters of ionic strength, volume fraction, and solvent evaporation temperature in vertical deposition (Tan et al, 2010).

3.2.1 Stick-slip behavior of colloidal deposition

When the positive polystyrene colloids are self-assembled on a negatively charged substrate, a uniform array of alternating linear patterns is usually obtained with limited widths (Ray et al 2005; Tan et al, 2010). As shown in Fig. 9, these 1D particulate bands are deposited at relatively regular intervals across the entire substrate. A magnified view of SEM photos reveals close-packed ordering within each band. However, the ordering quality is poor with abundant point and planar defects.

This alternating band is no different to the case of negatively charged particles being self-assembled on glass surface of same charge (Teh et al, 2004). The only difference is the presence of tiny clusters scattered within the so called "empty band" region. As discussed by Teh, the alternating bands can be attributed to the stick-slip motion of meniscus growth front during deposition, while the presence of scattered clusters in the "empty bands" could be caused by electrostatic attractions between colloids and substrate. Since the surface charge density of silica glass was determined to be -0.32mC/m^2 (Behrens & Grier, 2001), strong electrostatic attraction will immobilize positive particles if they happen to come close to the glass surface. This could explain the disordered random ordering of positive colloids in the "empty-band" region.

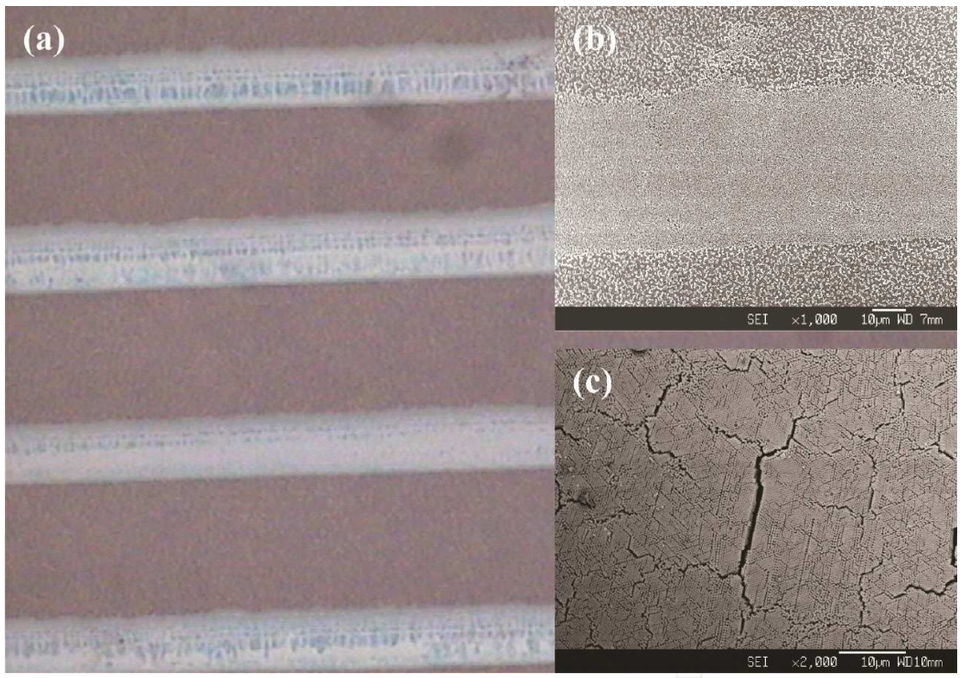

Fig. 9. (a) Microscopic picture shows interplay of stick-slip deposition and attractive deposition of positive colloids on negatively charged glass surface. (b) and (c) are magnified SEM photos showing alternating bands of ordered region and scattered clusters of random ordering. Particle concentration = 0.5 vol%, temperature = 35^{o}C. Reprinted with permission from *Langmuir*, Vol. 26, No. 10 (May 2010), pp. 7093-7100. Copyright 2010 American Chemical Society.

At the pinned contact line of meniscus, meniscus will first recede and deform with the consistent withdrawal of solvent in flow-controlled vertical deposition. Then the continual flux of particles to the thinning region will increase the local volume fraction and decrease

interparticle distance, causing the ordering to nucleate in the confined meniscus. If the meniscus thickness is larger than one particle diameter and recedes much slower than particle deposition, multilayer band with hcp orientation will be obtained. When the solution recedes further with contact angle reaching the minimum receding angle, the meniscus contact line will slip rapidly to a lower pinning level with a new contact angle. This process is then repeated with dynamic change of angle and alternating bands of deposition. More details can be found in Teh's published work (Teh et al, 2004).

3.2.2 Effect of volume fraction and ionic strength

Multilayer colloidal crystal shown in Fig. 9 was obtained with 0.5 vol% of colloidal suspension at 35^{o}C. When a more dilute concentration of 0.1 vol% was used (not shown), multilayered bands can be replaced by monolayers with locally ordered configurations. This can be explained by the lower particle flux to the drying edge during deposition, at the same withdrawal rate of suspension. At the same time, longer time is required for colloids to reach threshold concentration in the confined thin meniscus, implying that particles will have sufficient time to self-assemble in an orderly manner. Larger interparticle distance and lower frequency of collision due to Brownian motion are believed to slow down irreversible aggregation and random electrostatic adsorption of particles onto charged substrate. Hence, lower volume fraction of colloidal suspension is normally used to obtain long-range ordered crystal as slow increment of local volume fraction at thin meniscus is expected to impart greater inplane colloidal mobility during assembly process. Another comparison of concentration effect (0.05 and 0.01 vol%) on monolayer crystalline quality is given in Fig. 10. Dilution leads to better ordering quality, in agreement with other work (Zhou & Zhao, 2004).

Besides volume fraction, inplane mobility is also affected by electrostatic interaction between ordering particles in thin meniscus layer (Maskaly, 2006; Tan et al, 2008). For positive colloids, addition of salt (ionic strength increases) will reduce Debye screening length of the electric double layer. The result of this is twofold. First, positive colloids of similar charge will approach each other closer, and can be configured into stable in-plane ordered array with minimal cracks upon drying. Second, shorter Debye length will give positive colloids extra time to form ordered array, before being adsorbed onto negatively charged surface by electrostatic attraction. For example, the addition of 10 μM KCl was reported to give highest density of hcp domains, further supported by the distinctive 6-fold coordinated diffraction spots of a hexagonal lattice (Fig. 10 b). Detailed evidence can be referred to the relevant publication (Tan et al, 2010).

Besides, Tan also postulated that the assembly of charged colloids may achieve an intricate balance between particle-particle repulsion and particle-substrate attraction, when a colloidal suspension of low volume fraction and low ionic strength is used. This is a condition where the particles are sufficiently far apart to reorient themselves into geometrically and thermodynamically favored close-packed arrangement.

Fig. 11 shows the phase behavior of positive polystyrene colloids assembled on a negative silica glass substrate at 25^{o}C, at various ionic strength and volume fraction. It indicates that aggregates are likely to occur at high ionic strength across the whole studied range of volume fractions (0 to 0.1 vol%). For low ionic strength (< 10μM), long-range hcp ordering could be obtained with the use of low volume fraction (< 0.6 vf%).

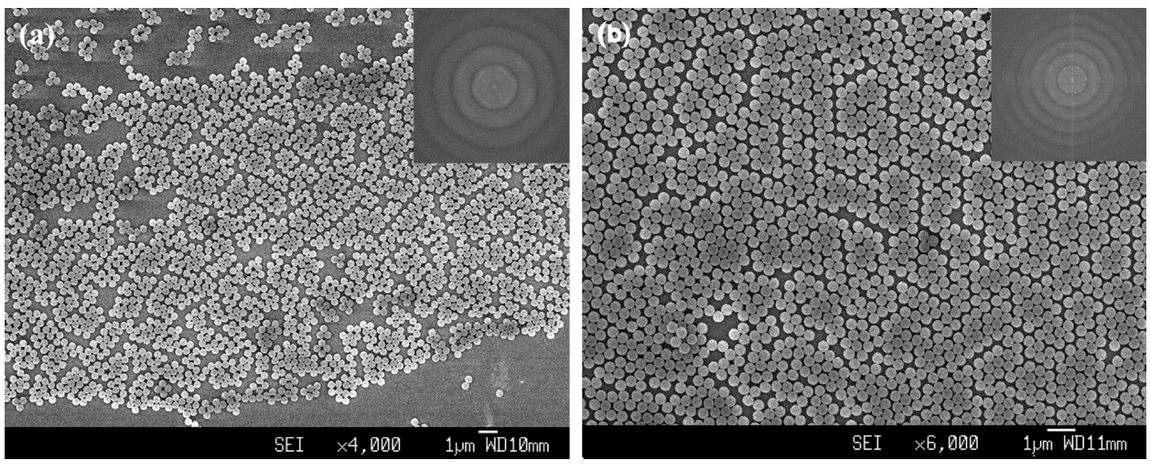

Fig. 10. Hexagonal close-packed domains and corresponding FFT inset obtained from vertical depositon at 25°C and 10 μM KCl. (a) Particle concentration = 0.05 vol % (b) Particle concentration = 0.01 vol%. Reprinted with permission from *Langmuir*, Vol. 26, No. 10 (May 2010), pp. 7093-7100. Copyright 2010 American Chemical Society.

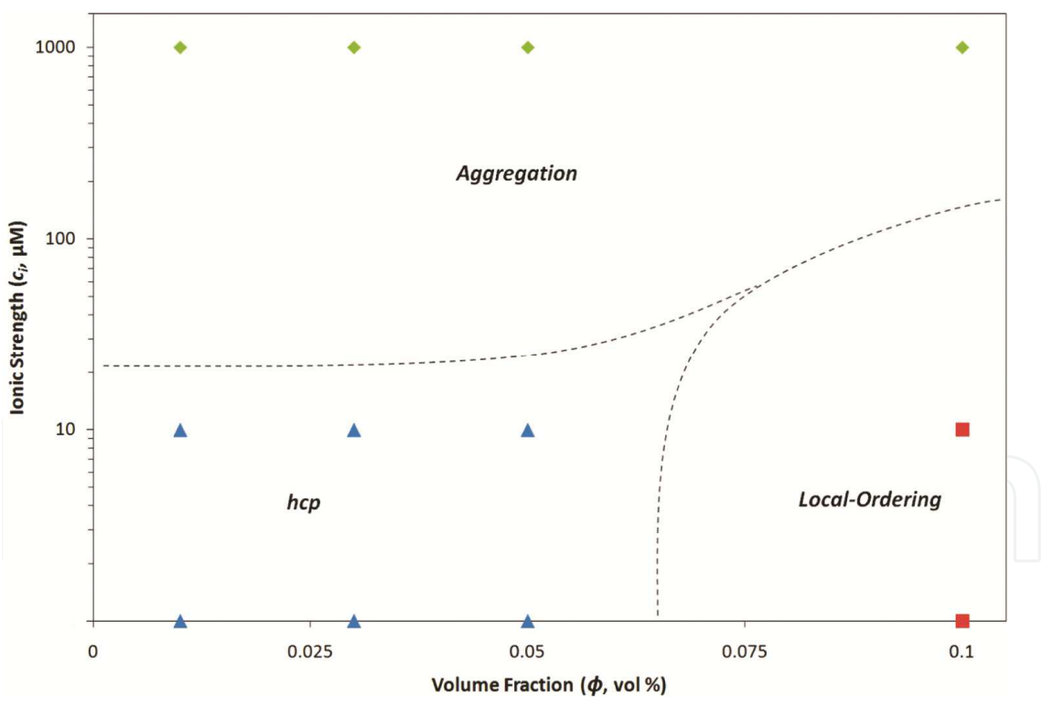

Fig. 11. Phase behavior of self-assembled colloidal structure, by deposition of positively charged polystyrene colloids on a negative borosilicate glass substrate at 25°C. Approximate boundaries between the ordered and glassy phases at different conditions are indicated by dashed lines. The axis of ionic strength is plotted in logarithm scale. Reprinted with permission from *Langmuir*, Vol. 26, No. 10 (May 2010), pp. 7093-7100. Copyright 2010 American Chemical Society.

3.2.3 Effect of temperature

There are two major effects brought by temperature increase (Dimitrov & Nagayama, 1996; McLachlan et al, 2004). First, high evaporation rate drives higher flux of particles to the drying edge, leading to faster crystal growth rate. Larger thickness of colloidal deposition is possible if solution withdrawal and meniscus deformation rate (thickness reduction) is much slower than particle flux. Second, kinetically active particles will bump into each other with high frequency. If they are of similar charge with substrate, higher ordering could be obtained since mobility is sufficiently large for further packing. However, substrate of opposite charge will likely immobilize colliding particles, giving no chance of good ordering (irreversible clustering).

3.2.4 Mobility in binary colloid

Earlier discussion has been devoted to the fine control of PS colloidal mobility in single-component crystallization. However, close-packed lattices have limited available symmetries (FCC or HCP) and associated properties which are too restrictive for diverse potential applications, especially in photonics. Using a mixed suspension of two particle types, colloidal crystals with lower symmetries can be made possible to provide novel properties in photonics, sensing and filtering (Bartlett et al, 1992; Kitaev & Ozin, 2003; Sharma et al, 2009; Tan et al, 2008).

Layer-by-layer growth is commonly used to self-assemble these structures, with right conditions of surfactants, temperature and ionic strength. Unlike the uniform negatively charged glass substrate used in self-assembly of positive colloids (see section 3.2.2), an underlying negatively charged L-colloidal template can be used to provide a periodic potential landscape to assist ordering of the next layer of colloids (named S-colloids) with opposite charge. These steps could be repeated to get additional layers of LS_n structures.

In LS_2 structures (see inset in Fig. 12a), each interstice in the first layer of hexagonally close packed (hcp) particles (L) is filled by one small particle (S). LS_6 structure is also possible where each interstice of first layer is filled by three particles (S) instead (Sharma et al, 2009). Unfortunately, both lower and higher densities of binary structures are usually observed together in LBL experiments. This led to an extended work to study the particulate mobility of colloids over an ordered potential landscape of an assembled hcp monolayer of opposite charge (Tan et al, 2010).

In previous work, Tan reported that a low ionic strength of 10 μM KCl could vastly improve the ordering of attractive binary colloidal structures in layer-by-layer (LbL) growth, presumably because the S-colloids possess sufficient mobility to self-assemble into a highly symmetrical LS_2 2D-superlattice. Besides ionic strength, crystalline quality also depends strongly on evaporation temperature and the most uniform LS_2 was obtained at low temperature (25°C). Fig. 13 shows a comparison of temperature effects (25°C vs 35°C) over LS_2 assembly using 10μM of KCl electrolyte. Similar to the case of single-component crystallization on glass surface of opposite charge, lower evaporation rate and slow crystal growth rate provide additional time for S-particles to reorient and stabilize into a thermodynamically favorable in-plane LS_2-superlattice (in suspension), before settling onto the oppositely charged template (L-layer). On the other hand, a slight increase of temperature to 35°C disrupts the inplane ordering structure, resulting in disordered binary arrays. This can be explained by greater Brownian motion of particles and faster loss of water due to evaporation, in which water is the key to mobility during ordering.

Thus a consensus can be drawn that an intricate balance of the particulate mobility by all three parameters, (1) evaporation temperature, (2) volume fraction, and (3) ionic strength, is critical for the quality of self-assembled colloidal crystals. Other than these, the delivery speed of the particles to crystal growth front should equal the crystal growth rate. These can be optimized by evaporation control and meniscus receding rate. Regardless of the type of substrates and the charge of particles used, particulate mobility must be assured to guarantee sufficient time of reordering to achieve final irreversible crystallization. Next we will discuss various templating efforts to obtain perfect single crystal and crystals with complex symmetry, which are impossible to be achieved by conventional self-assembly on bare substrates.

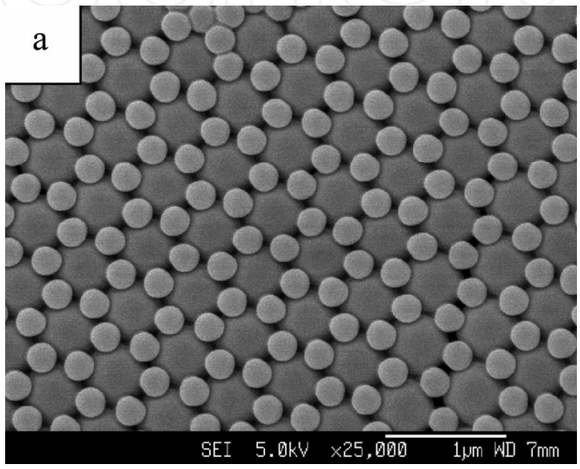

Fig. 12. Layer-by-layer assembly of positive colloids (250 nm) onto a hcp monolayer of negatively charged particles (550 nm) in flow-controlled vertical deposition, revealing LS_2 structure. Reprinted with permission from *Langmuir*, Vol. 26, No. 10 (May 2010), pp. 7093-7100. Copyright 2010 American Chemical Society.

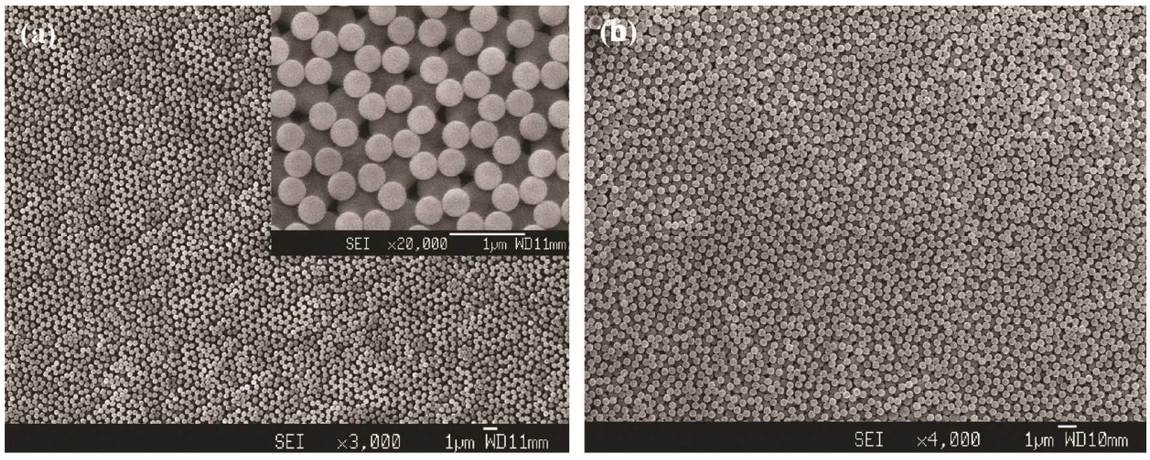

Fig. 13. Layer-by-layer assembly of positive colloids (371 nm) onto a hcp monolayer of negatively charged particles (604 nm) in flow-controlled vertical deposition, at temperature of (a) 25°C and (b) 35°C. Reprinted with permission from *Langmuir*, Vol. 26, No. 10 (May 2010), pp. 7093-7100. Copyright 2010 American Chemical Society.

4. Towards perfect crystallization

4.1 Template-assisted self-assembly

Despite many efforts to grow large-area perfect crystal (> 1000μm^3) that are useful for optical devices, most do not offer sound practicality for large scale integration. Sedimentation is extremely slow, limited by absence of control over number of layers and uniformity over topology. The method based on vertical deposition requires strict control of surface charge density of particles or substrate, particle and electrolyte concentration, temperature, and humidity.

Geometrical confinement has been long studied to affect the phase behavior of colloidal particle ordering (Schmidt & Löwen, 1997; Ramiro-Manzano et al, 2007). By using thin parallel plates or a wedge cell of few particle diameters in gap, crystal transitions (e.g. buckling) can be observed with changes of cell thickness. Similar confinement approach was also extended by Park et al to obtain much better ordering and orientation compared to the colloidal crystals grown from bare substrate (Park et al, 1997). Using pressure, they injected a suspension of colloidal particles into a well-confined rectangular cubic cell, with solvents being drained out through the channels (< particle diameter) built lithographically along the side walls of the cell. This left behind accumulating particles at the bottom of the cell and rapid crystallization of particles over 1 cm^2 with well-controlled number of layers (1 ~ 50 layers) could be easily attained. With sonication (Sasaki & Hane, 1996), the packing quality of close-packed lattice could be further improved under flow. This cell can then be dried off in an oven and dismantled later. The perfect colloidal crystal confined by these physical walls could then be integrated into device-making. Crytals grown this way have 3D domain size of 12 μm x 0.5 cm x 2 cm, which is almost equivalent to the cell size of 12μm x 2 cm x 2cm.

Coupling with the laminar flow of colloidal particles, flow-driven organization of particles in microchannels (rectangular grooves) was studied (Kumacheva et al, 2003). Using template with periodic rectangular grooves, the influence of the width and size of such rectangular grooves on colloidal self-assembly was investigated. Depending on the commensurability of the particle into the grooves, various structures like close-packed hexagonal, rhombic and disordered structures were reported. If a large mismatch (> 15%) exists between the ideal and experimental ratios, defects would be introduced in the crystal structure. In a subsequent study, a much narrower groove was explored, in which only parts of a colloidal sphere could (snugly) fit into. Precise ordering of colloidal lines was thus obtained (Allard et al, 2004).

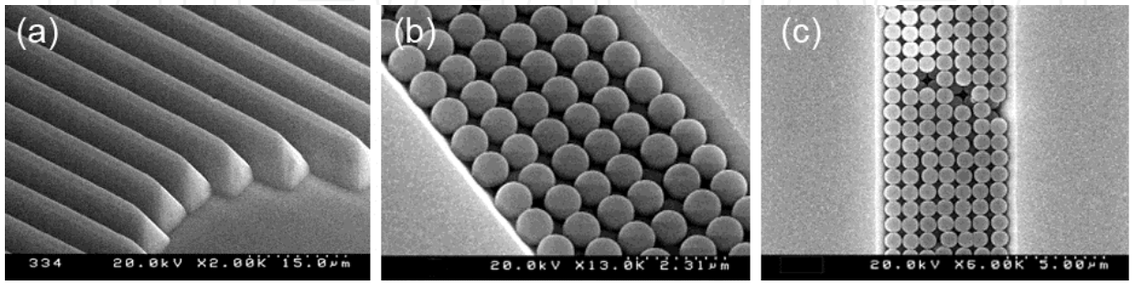

Fig. 14. (a) Anisotropically etched V-shaped channels into a Si (100) wafer obtained using lithography. (b) SEM photo depicts six-layer (100) single crystal made of silica particles, sitting in a V-grooved channel. (c) Vacancy defects observed in the top layer of micro-spheres. (Yang & Ozin, 2000) – Reproduced by permission of The Royal Society of Chemistry.

In order to enable realization of colloidal crystals in devices, they must be fabricated into planarized microphotonic crystal chips. Ozin and his group pioneered the fabrication of planarized microphotonic structures by the deposition of micro-spheres into V-shaped grooves (apex angle = 70.6^{o}) (Ozin & Yang, 2000 & 2001). The nucleation was believed to first occur along the apex of the V-grooves, followed by the subsequent layers of growth. The depth of such grooves will determine the number of layers of colloidal crystal formed and the close-packing tendency ensures projection of (100) crystal orientation, terminating at the crystal-air interface (see Fig. 14).

Emerging micro- and nanofabrication technologies in template structuring allows one to shrink the pattern size to tens of nanometers (e.g. e-beam lithography). The ability to create nano- or microfeatures consistently enables precise deposition of each particle and control over its packing symmetry, packing efficiency and packing quality of the resulting crystal. Using topologically patterned templates, Van Blaaderen et al showed that slow sedimentation of colloidal particles into the ''holes'' of topologically patterned templates enables formation of fcc colloidal crystals with crystal orientation of (100) planes parallel to the patterned surface (Blaaderen et al, 1997). This is different from the usual (111) plane orientation obtained, with respect to the surface. They succeeded to achieve large oriented crystals at which the defect structures were tailored by surface graphoepitaxy[2] approach. As the template used has a known orientation, photonic crystals grown could be sliced such that the exposed (001) and (110) facets of the fcc crystal structure could be integrated into specific applications. It was also shown that intentional mismatch of hole pitch and particle diameter can give rise to defect structures, such as randomly stacked (111) planes above the first few layers from the surface of template. This is similar to the case of growing epitaxial layer of CdTe (111) on GaAs (001) substrate, with a mismatch of about 14.6% (Bourret et al, 1993). Other than this, other cubic packing system like body-centered cubic (bcc) and simple cubic (sc) colloidal crystals have also been reported using similar approach (Hoogenboom et al, 2004).

It is obvious that templating offers a remedy to the shortcomings of spontaneous colloidal self-assembly, especially in manufacturing crystals tailored for realistic photonic applications. Other than the potential to obtain defect-free colloidal crystal of fcc structure with different plane orientation, it is also possible to assemble monodisperse colloids into complex structures or subunits (Romano & Sciortino, 2011; Vinothan et al, 2003), and then lead them to complex crystal symmetries of lower packing density.

According to photonic band structures calculated for various crystal symmetries and dielectrics (Ho et al, 1990; Pradhan et al, 1997; Busch & John, 1998; Moroz & Sommers, 1999; Vlasov et al, 2000), it was confirmed that an fcc colloidal structure has a PBG only in the second Brillouin zone (second-order Bragg diffraction), not in the first Brillouin zone (Blanco et al, 2000). Besides, a sufficiently high refractive index contrast (> 2.8) between the building blocks of the fcc crystal (colloidal particles and the interparticle space) is required to obtain a full omnidirectional band gap. Furthermore, photonic properties of commonly found fcc crystals are very sensitive to structural disorder (Vlasov et al, 2000). In this regard, nonspherical particles also offer immediate advantages in applications that require lattices with lower symmetries and higher complexities.

[2] Growth of crystal by substrate topology as opposed to atomic lattice in which a material is crystallized onto an existing crystal of another material, resulting in effective continuation of the crystal structure of the substrate.

Templates used for "nucleation" of complex colloidal clusters or crystal layers are usually engineered by modification of the surfaces via lithography (Chen et al, 2000; Choudhury, 1997; Rijn et al, 1998) and chemical patterning (Bertrand et al, 2000; Delamarche et al, 1998; Ulman, 1996; Xia & Whitesides, 1998). The control of surface chemistry like charge and functional reactivity can be obtained by coating an adhesive monolayer which is specific to the substrate, called self-assembled monolayers (SAM) (Ulman, 1996). For example, one can use thiol functional groups for gold surface, and silanes for silica substrate. The functional groups of this self-assembled molecular layer will then adhere to the corresponding surface with the other desired ends (e.g. charge for particle interactions) projected outwards. Besides, one can also use SAMs to coat different charges (positive, negative or neutral) on each crystal layer grown via layer-by-layer method to obtain binary colloidal crystal in vertical deposition.

Other than direct photolithography or e-beam lithography to create paterns on these SAM layers, SAM patterns can also be transferred to a flat substrate by soft lithography (Xia & Whitesides, 1998) and nanoimprint lithography (Hu & Jonas, 2010; Torres, 2003). Subsequent ordering of colloidal particles on such chemically defined patterns can be achieved in vertical deposition via electrostatic interaction and capillary forces. As discussion in section 3.2, charged microspheres can be self-assembled on the oppositely charged areas of the patterns when the substrate is slowly taken out from the colloidal suspension (Fustin et al, 2004). Depending on the size ratio of colloidal particle and patterned area, complex colloidal aggregates can be grown (Lee et al, 2002).

Despite progressive advancements in lithography systems, high facility cost and maintenance impede practical use of templating in colloidal self assembly. Hence, it is worth exploring simple templating like V-groove, and low-cost templating system like soft lithography and nanoimprinting, to enable innovative ways for template-assisted self-assembly. Next, we will discuss our approach to utilize meniscus pinning to control positional nucleation and inplane-oriented growth of large area monolayer colloidal crystal from one straight surface relief.

4.2 Controlling inplane orientation of large area monolayer colloidal crystal

Among various top-down and bottom-up methods discussed earlier, capillary forces induced convective self-assembly is attractive, requiring only a simple and economical setup. However, common nonidealities like thickness nonuniformity, restricted domain size and empty bands or voids are frequently reported. When a substrate is submerged into a liquid, a wavy contact line is commonly observed at air-liquid-solid interface, due to Rayleigh instability (Davis, 1980). In vertical deposition, it is believed that the trapping of colloidal particles along this wavy contact line will first lead to accumulation of particles, and then multidirectional initiation of colloidal crystal growth (Fig. 15c). Since the domain growth directions tend to be different along the wavy contact line; this eventually limits the final domain size of colloidal crystals obtained. Other than this, dynamic change of receding contact angle of colloidal suspension during liquid or substrate withdrawal will produce colloidal stripes or alternating colloidal and empty bands via the stick-slip mechanism (Adachi et al, 2005; Teh, 2004; Thomson et al, 2008).

Here, we demonstrate the usage of meniscus pinning by surface relief boundaries to control in-plane orientation of monolayer colloidal crystals without the interruption of grain disorientation. By printing a straight surface relief which has a strong affinity to water

molecules (common solvent for colloidal particles), a straight wetting line of colloidal suspension could be pinned along the surface relief patterned (Fig. 15a). The photoresist SU-8 has been shown to work in this context. As most photoresists do not have good affinity to water (hydrophobic), their surface can be treated with UV ozone to improve wetting. A small addition of surfactant (SDS) and trapping of colloidal particles along wetting line do give enhanced pinning by almost 100%.

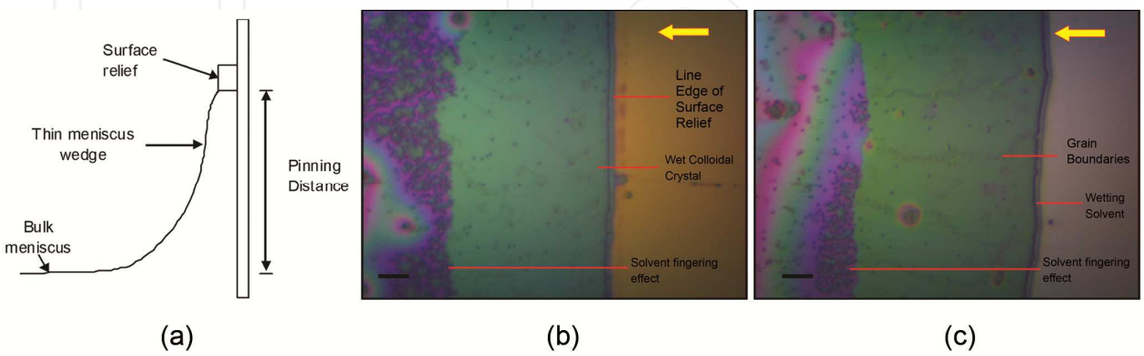

Fig. 15. (a) Schematic shows how water film is pinned and stretched near surface relief when the substrate is being pulled out of colloidal suspension. (b) Optical micrograph shows straight liquid pinning and nucleation along surface relief, and the subsequent inplane oriented growth. (c) Optical micrograph shows that colloidal nucleation on bare substrate always starts with wavy contact line and wavy nucleation line, giving rise to polydomain growth. As indicated, fingering effect of wetting solvent is observed above the wet assembled colloidal crystal. Yellow arrows show liquid receding direction. The scale bar is 8μm. Reprinted with permission from *Langmuir*, Vol. 27, No. 6 (March 2011), pp. 2244-2249. Copyright 2011 American Chemical Society.

The initial establishment of liquid pinning along straight surface relief will allow colloidal particle deposition along the thin meniscus wedge (Fig. 15b). Fast substrate withdrawal or receding bulk meniscus relative to colloidal deposition speed will pull the pinned contact line, either causing depinning or contact-line movement in a fingering pattern (Sharma & Reiter, 1996; Troian et al, 1989), together with the pinned colloidal domains. Hence, depinning of the initial contact line must be avoided.

By optimizing the pinning boundary and withdrawal speed, a well-controlled linear meniscus contact line allows a straight nucleation edge of monolayer crystal growth front, which then acts as a crystal growth seed, permitting the most close-packed direction <11> or <10> (as in 2D hexagonal lattice) to assemble along the surface relief. As a result, this unidirectional growth can give rise to single domain crystals with only twins and vacancies present as residual defects (see Fig. 16). More evidence can be referred to the supporting documents provided at the publication site (Ng et al, 2011).

Conservatively, the domain crystal size obtained can be as large as 1 mm^2, with residual defects of vacancies, twin boundaries and small misoriented domains. Despite these imperfections, the domain orientation of large crystal domain remains similar. More evidence in the form of SEM photos scanned sequentially can be found in the supporting documents published (Ng et al, 2011). To conclude, this novel approach could offer the desired ease of integration for device making, as the inplane-orientation of crystal grown can be easily identified by referring to the engineered surface relief.

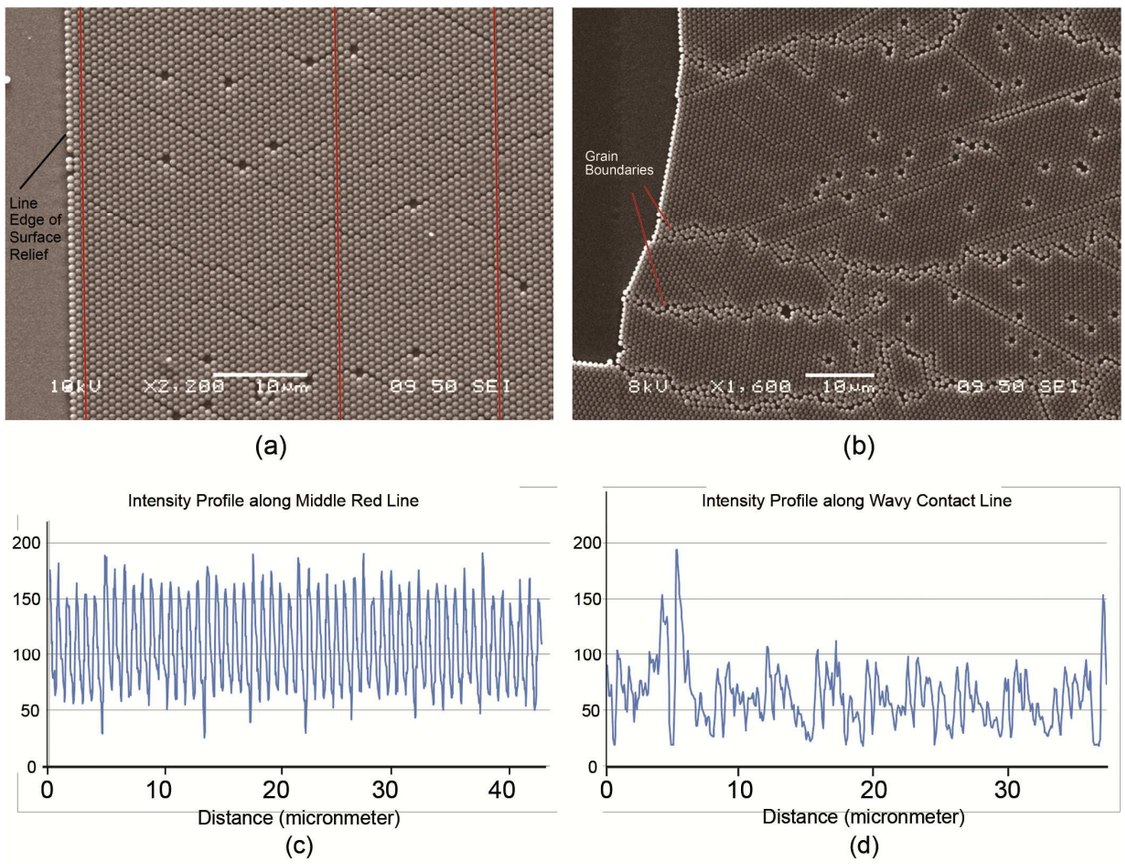

Fig. 16. SEM photo (a) shows inplane domain-oriented growth of colloidal crystal from the edge of straight surface relief, producing high degree of directionality. Particles are lined up in the close-packed direction <10> or <11>, along the surface relief. Red lines drawn serve as a guide to illustrate the perfect orientation under the straight pinning effect. (b) For comparison, colloidal assembly on bare substrate is shown, explaining the effect of wavy lines which result in domain growth of various directions. The desired growth directions are from left to right. (c) and (d) show line-plot profiles generated using ImageJ[3], along middle red line in part a and across central region in part b, respectively. Reprinted with permission from *Langmuir*, Vol. 27, No. 6 (March 2011), pp. 2244-2249. Copyright 2011 American Chemical Society.

5. Characterization of colloidal crystal

The most commonly used modern instruments in imaging dried colloidal crystals are scanning electron microscope (SEM) and transmission electron microscope (TEM). These types of imaging provide a quick view on the periodic structures grown via colloidal self-assembly; it does not however give quantitative data like crystal parameters in three dimensions. They are only good for 2D and topology scanning with smaller field of view

[3] ImageJ is a Java application popular for SEM and TEM image processing and analysis. More on http://rsbweb.nih.gov/ij/

(short range). If the particles are large enough (> 1μm diameter), their motion and ordering can also be observed with optical microscopes (Denkov et al, 1992; Pieranski, 1983; Yan et al, 2008).

Fortunately, the ability of colloidal crystal to diffract light allows one to characterize the crystal structure and quality with ease (Hiltner & Krieger, 1969). For colloidal crystals with lattice spacings in the order of visible-light wavelengths, diffraction method can be used in transmission mode or reflectance mode (Imura et al, 2009; Koh et al, 2006). As discussed earlier, in order for electromagnetic waves to diffract, it must obey the following Bragg's law. Direct reflection peak or transmission peak can then be recorded using UV-vis spectrometer.

$$\lambda = 2n_{eff}d_{111} \tag{4}$$

$$n_{eff} = \sqrt{(\Psi n_{ps}^2 + (1-\Psi)n_{air}^2} \tag{5}$$

$$d_{111} = (\frac{2}{3})^{\frac{1}{2}}D \tag{6}$$

where n_{eff} is effective refractive index of the colloidal suspension, d_{111} is the interlayer spacing between (111) plane, D is particle diameter, n_{ps} and n_{air} are refractive indices of polystyrene particle and air respectively, and ψ is the volume fraction of particles in suspension.

Unfortunately, strong interaction between light and the crystals could result in multiple scattering. It was observed that the Bragg spacings derived from diffraction measurements could deviate strongly from the real lattice spacings (Los et al, 1996). Besides, the available optical spectrum limits the number of Bragg reflections to be observed. These issues could be remedied by small angle X-ray scattering. First, X-ray interacts weakly with colloidal particles, serving as an excellent tool to probe internal structure of photonic crystal. Second, since there is a dramatic difference between X-ray wavelength (~1Å) and the particle diameter (e.g. 1μm), a tiny diffraction angle (narrow focus range) in the order of 10^{-4} rad will be able to supply sufficient information regarding the crystal (Thijssen et al, 2006). To conclude, radius, size distribution and internal structure of particle, crystal structure, lattice parameter and average orientation of colloidal crystal can be investigated via X-ray scattering (Megens et al, 1997; Vos et al, 1997).

Kossel lines, previously used in X-ray diagrams or electron diffraction experiments (Kikuchi lines) had also been used to examine phase transformation of colloidal crystal, crystal structures and their lattice parameters (Clark et al, 1979; Pieranski et al, 1981; Yoshiyama et al, 1984). Fig. 17 demonstrates a simple setup to obtain Kossel diagram, which is either projected on a spherical screen, V or a flat one, F. The colloidal crystal suspension is held in a glass or quartz cuvette, which is immersed in a spherical vessel V (diameter ~ 10 cm) filled with pure water. This water-filled vessel serves to minimize the refraction at the surface of the crystal. A divergent laser beam (normally He-Ne, λ = 632.8 nm) is then focused through a window and the diffracted beam will be projected on the spherical projection screen V or on a flat screen at distance X.

It should be noted that a 2D map of diffraction spots could be printed on the projected screen in Fig. 17, if a collimated white light is used. This offers a distinct advantage in

immediate identification of the wavelength diffracted, based on the colour of the projected Laue spots. Other than white light, collimated laser and X-rays can also be used to obtain diffraction spots, by vary the scanning angle of the incoming beam (Williams & Crandall, 1974; Clark & Hurd, 1979).

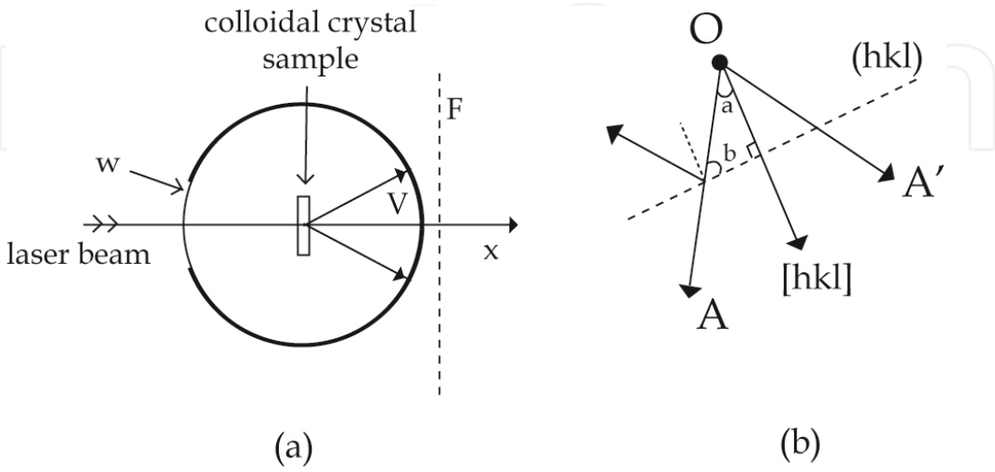

Fig. 17. (a) Experimental set-up of Kossel analysis, where a divergent laser beam is shone through thin colloidal crystal sample and the diffracted beam is projected on the curved screen V or flat screen F. (b) Diagram shows formation of Kossel cone in (a), where the Kossel lines are the intersection between the Kossel cone and the projection screen shown in (a). (Pieranski et al, 1981)

6. Conclusion

In spite of recent progress in colloidal self-assembly, large scale ordering of colloidal crystals with controlled packing symmetry, periodicity, crystal orientation and packing quality in a practical and economical application still remains an active scientific and engineering activity. This interest is intensively fuelled by the many fundamental scientists, application engineers and researchers working in tailored colloidal crystals exhibiting novel functions in applications. This chapter highlights not only our own work in colloidal self-assembly, but also the fundamental concepts and key approaches used to grow colloidal crystals. We think that particle-particle interactions in the process of assembly, mobility and space confinement remain the three crucial keys in fabricating performance-sound colloidal crystals.

For example, one could think of giving directional properties to colloidal particles and control the particle interactions in short range to form tetrahedral clusters. The clusters can then be directed into long range assembly via necessary confinement (e.g. meniscus, template, etc) to achieve equilibrium ordering of a diamond lattice. Simulations can also be deployed to assess the feasibility of related colloidal crystal structures for specific tailored synthesis, assembly and performance. However, the common inherent problem remains over the practicalities: speed, cost, area of crystal grown and ease of integration. In conclusion, the potential is huge, and there is still much room for future research.

7. Acknowledgment

We acknowledge all the works contributed by our group members, including those who have left for good cause. They are Mr. Tan Kwan Wee, Dr. Yan Qing Feng, Dr. Teh Lay Kuan and Dr. Yip Chan Hoe. We also thank Singapore-MIT alliance for the funding support throughout the years.

8. References

Adachi, E., Dimitrov, A. S. & Nagayama, K. (1995). Stripe Patterns Formed on a Glass Surface during Droplet Evaporation. *Langmuir,* Vol.11, No.4, (April 1995), pp. 1057-1060

Allard, M., Sargent, E. H., Lewis, P. C. & Kumacheva, E. (2004). Colloidal Crystals Grown on Patterned Surfaces. *Advanced Materials,* Vol.16, No.15, (August 2004), pp. 1360-1364

Arora, A. K. & Tata, B. V. R. (1996). *Ordering and Phase Transitions in Charged Colloids* (1st ed), Wiley-VCH, ISBN 0471186309

Auer, S. & Frenkel, D. (2001). Prediction of Absolute Crystal-nucleation Rate in Hard-sphere Colloids. *Nature,* Vol.409, No.6823, (February 2001), pp. 1020-1023

Avrutsky, I., Kochergin, V. & Zhao, Y. (2000). Optical Demultiplexing in a Planar Waveguide with Colloidal Crystal. *IEEE Photonics Technology Letters,* Vol.12, No.12, (December 2000), pp. 1647-1649

Bartlett, P., Ottewill, R. H. & Pusey, P. N. (1992). Superlattice Formation in Binary Mixtures of Hard-sphere Colloids. *Physical Review Letters, Vol.*68, No.25, (June 1992), pp. 3801-3805

Behrens, S. H. & Grier, D. G. (2001). The Charge of Glass and Silica Surfaces. *The Journal of Chemical Physics.* Vol.115, No.14, (2001), pp. 6716-6721

Bertrand, P., Jonas, A., Laschewsky, A. & Legras, R. (2000). Ultrathin Polymer Coatings by Complexation of Polyelectrolytes at Interfaces: Suitable Materials, Structure and Properties. *Macromolecular Rapid Communications,* Vol.21, No.7, (April 2000), pp. 319-348

Biró, L. P., Bálint, Z., Kertész, K., Vértesy, Z., Márk, G. I., Horváth, Z. E., Balázs, J., Méhn, D., Kiricsi, I., Lousse, V. & Vigneron, J. P. (2003). Role of Photonic-crystal-type Structures in the Thermal Regulation of a Lycaenid Butterfly Sister Species Pair. *Physical Review E,* Vol.67, No.2, (February 2003), pp. 021907-1 – 021907-6

Blanco, A., Chomski, E., Grabtchak, S, Ibisate, M., John, S., Leonard, S., Lopez, C., Meseguer, F., Miguez, H, Mondian, J. Orzin, G. A., Toader, O. & van Driel, H. M. (2000). Large-scale Synthesis of a Silicon Photonic Crystal with a Complete Three-dimensional Bandgap near 1.5 Micrometres. *Nature,* Vol.405, No.6785, (May 2000), pp. 437-440

Bourret, A., Fuoss, P., Feuillet, G. & Tatarenko, S. (1993). Solving an Interface Structure by Electron Microscopy and X-ray Diffraction: The GaAs(001)-CdTe(111) Interface. *Physical Review Letters,* Vol.70, No.3, (January 1993), pp. 311-315

Busch, K. & John, S. (1998). Photonic Band Gap Formation in Certain Self-organizing Systems. *Physical Review E,* Vol.58, No.3, (September 1998), pp. 3896-3908

Chen, K. M., Jiang, X., Kimerling, L. C. & Hammond, P. T. (2000). Selective Self-Organization of Colloids on Patterned Polyelectrolyte Templates. *Langmuir,* Vol.16, No.20, (October 2000), pp. 7825-7834

Chen, M., Kim, J., Liu, J. P., Fan, H. & Sun, S. (2006). Synthesis of FePt Nanocubes and Their Oriented Self-Assembly. *Journal of the American Chemical Society,* Vol.128, No.22, (June 2006), pp. 7132-7133.

Clark, N. A., Hurd, A. J. & Ackerson, B. J. (1979). Single Colloidal Crystals. *Nature,* Vol.281, No.5726, (September 1979), pp. 57-60

Crandall, R. S., & Williams, R. (1977). Gravitational Compression of Crystallized Suspensions of Polystyrene Spheres. *Science,* Vol.198, No.4314, (October 1977), pp. 293-295

Davis, S. H. (1980). Moving Contact Lines and Rivulet Instabilities. Part 1. The Static Rivulet. *Journal of Fluid Mechanics,* Vol.98, No.2, (1980), pp. 225-242

Delamarche, E., Schmid, H., Bietsch, A., Larsen, N. B., Rothuizen, H., Michel, B. & Biebuyck, H. Transport Mechanisms of Alkanethiols during Microcontact Printing on Gold. *The Journal of Physical Chemistry B,* Vol.102, No.18, (April 1998), pp. 3324-3334

Denkov, N., Velev, O., Kralchevski, P., Ivanov, I., Yoshimura, H. & Nagayama, K. (1992). Mechanism of Formation of Two-dimensional Crystals from Latex Particles on Substrates. *Langmuir,* Vol.8, No.12, (December 1992), pp. 3183-3190

Dushkin, C. D., Yoshimura, H. & Nagayama, K. (1993). Nucleation and Growth of Two-dimensional Colloidal Crystals. *Chemical Physics Letters,* Vol.204, No. 5-6, (March 1993), pp. 455-460

Fustin, C., Glasser, G., Spiess, H. W. & Jonas, U. (2004). Parameters Influencing the Templated Growth of Colloidal Crystals on Chemically Patterned Surfaces. *Langmuir,* Vol.20, No.21, (October 2004), pp. 9114-9123

Gasser, U., Weeks, E. R., Schofield, A., Pusey, P. N. & Weitz, D. A. (2001). Real-Space Imaging of Nucleation and Growth in Colloidal Crystallization. *Science,* Vol.292, No.5515, (April 2001), pp. 258 -262

Gast, A. P. & Russel, W. B. (1998). Simple Ordering in Complex Fluids. *Physics Today,* Vol.51, No.12, (1998), pp. 24-30

Habdas, P. & Weeks, E. R. (2002). Video Microscopy of Colloidal Suspensions and Colloidal Crystals. *Current Opinion in Colloid & Interface Science,* Vol.7, No.3-4, (August 2002), pp. 196-203

Hales, T. C. (1997). Sphere packings, I. *Discrete & Computational Geometry,* Vol.17, No.1, (January 1997), pp. 1-51

Hiltner, P. A. & Krieger, I. M. (1969). Diffraction of Light by Ordered Suspensions. *The Journal of Physical Chemistry,* Vol.73, No.7, (July 1969), pp. 2386-2389

Ho, K. M., Chan, C. T. & Soukoulis, C. M. (1990). Existence of a Photonic Gap in Periodic Dielectric Structures. *Physical Review Letters*, Vol.65, No.25, (December 1990), pp. 3152-3155

Holgado, M., García-Santamaría, F., Blanco, A., Ibisate, M., Cintas, A., Míguez, H., Serna, C. J., Molperceres, C., Requena, J., Mifsud, A., Meseguer, F. & López, C. Electrophoretic Deposition To Control Artificial Opal Growth. *Langmuir,* Vol.15, No.14, (July 1999), pp. 4701-4704

Hoogenboom, J. P., Rétif, C., de Bres, E., van der Boes, M., van Langen-Suurling, A. K. & Romijn, J. (2004). Template-Induced Growth of Close-Packed and Non-Close-Packed Colloidal Crystals during Solvent Evaporation. *Nano Letters,* Vol.4, No.2, (February 2004), pp. 205-208

Hoover, W. & Ree, F. (1968). Melting Transition and Communal Entropy for Hard Spheres. *The Journal of Chemical Physics,* Vol.49, No.8, (October 1968), pp. 3609-3617, ISSN 00219606

Hu, Z. & Jonas, A. M. (2010). Control of Crystal Orientation in Soft Nanostructures by Nanoimprint Lithography. *Soft Matter,* Vol.6, No.1, (2010), pp. 21-28

Im, S. H., Kim, M. H. & Park, O. O. (2003). Thickness Control of Colloidal Crystals with a Substrate Dipped at a Tilted Angle into a Colloidal Suspension. *Chemistry of Materials* Vol.15, No.9 (May 2003), pp. 1797-1802

Imura, Y., Nakazawa, H., Matsushita, E., Morita, C., Kondo, T. & Kawai, T. (2009). Characterization of Colloidal Crystal Film of Polystyrene Particles at the Air-Suspension Interface. *Journal of Colloid and Interface Science,* Vol.336, No.2, (August 2009), pp. 607-611

Jiang, P., Bertone, J. F., Hwang, K. S., Colvin, V. L. (1999). Single-Crystal Colloidal Multilayers of Controlled Thickness. *Chemistry of Materials*, Vol.11, No.8, (1999), pp. 2132-2140

Jiang, P. & McFarland, M. J. (2004). Large-Scale Fabrication of Wafer-Size Colloidal Crystals Macroporous Polymers and Nanocomposites by Spin-Coating. *Journal of the American Chemical Society,* Vol.126, No.42, (October 2004), pp. 13778-13786

Kay, L. E. (1986). W. M. Stanley's Crystallization of the Tobacco Mosaic Virus, 1930-1940. *Isis,* Vol.*77*, No.3, (September 1986), pp. 450-472

Kitaev, V. & Ozin, G. A. (2003). Self-Assembled Surface Patterns of Binary Colloidal Crystals. *Advanced Materials,* Vol.15, No.1, (January 2003), pp.75-78

Koh, Y. K. & Wong C. C. In Situ Monitoring of Structural Changes during Colloidal Self-Assembly. *Langmuir,* Vol.22, No.3, (January 2006), pp. 897-900

Koh, Y. K., Yip, C. H., Chiang, Y. M. & Wong, C. C. (2008). Kinetic Stages of Single-Component Colloidal Crystallization. *Langmuir* Vol. 24, No. 10 (May 2008), pp. 5245-5248

Kralchevsky, P. A. & Nagayama, K. (1994). Capillary Forces between Colloidal Particles. *Langmuir,* Vol.10, No.1, (January 1994), pp. 23-36

Kralchevsky, P. A. & Denkov, N. D. (2001). Capillary Forces and Structuring in Layers of Colloid Particles. *Current Opinion in Colloid & Interface Science,* Vol.6, No.4, (August 2001), pp. 383-401

Kumacheva, E., Garstecki, P., Wu, H. & Whitesides, G. M. (2003). Two-Dimensional Colloid Crystals Obtained by Coupling of Flow and Confinement. *Physical Review Letters,* Vol.91, No.12, (September 2003), pp. 128301-1 –128301-4

Lee, I., Zheng, H., Rubner, M. F. & Hammond, P. T. (2002). Controlled Cluster Size in Patterned Particle Arrays via Directed Adsorption on Confined Surfaces. *Advanced Materials,* Vol.14, No.8, (April 2002), pp. 572-577

Lee, K. H., Chen, Q. L., Yip, C. H., Yan, Q. & Wong, C. C. (2010). Fabrication of Periodic Square Arrays by Angle-resolved Nanosphere Lithography. *Microelectronic Engineering,* Vol.87, No.10, (October 2010), pp. 1941-1944

Liu, J. (2005). *Photonic devices,* Cambridge University Press, ISBN 0521551951

Lu, Y., Yin, Y. & Xia, Y. (2001). Preparation and Characterization of Micrometer-Sized 'Egg Shells'. *Advanced Materials,* Vol.13, No.4, (February 2001), pp. 271-274

Manoharan, V., Elsesser, M & Pine, D. J. (2003). Dense Packing and Symmetry in Small Clusters of Microspheres. *Science,* Vol.301, No.5632, (July 2003), pp. 483-487

Maskaly, G. R., García, R. E., Carter, W. C. & Chiang, Y. M. (2006). Ionic Colloidal Crystals: Ordered, Multicomponent Structures via Controlled Heterocoagulation. *Physical Review E,* Vol.73, No.1, (January 2006), pp. 011402-1 – 011402-8

Mayoral, R., Requena, J., Moya, J., López, C., Cintas, A., Miguez, H., Meseguer, F., Vásguez, L., Holgado, M. & Blanco, A. (1997). 3D Long-range ordering in an SiO_2 Submicrometer-sphere Sintered Superstructure. *Advanced Materials,* Vol.9, No.3 (March 1997), pp. 257-260

Megens, M., van Kats, C. M., Bösecke, P. & Vos, W. L. (1997). Synchrotron Small-Angle X-ray Scattering of Colloids and Photonic Colloidal Crystals. *Journal of Applied Crystallography,* Vol.30, No.5-2, (October 1997), pp. 637-641

McLachlan, M. A., Johnson, N. P., Rue, R. M. & McComb, D. W. (2004). Thin Film Photonic Crystals: Synthesis and Characterisation. *Journal of Materials Chemistry,* Vol.14, No.2, (2004), pp. 144-150

Míguez, H., Meseguer, F., López, C., Mifsud, A., Moya, J. S. & Vázquez, L. (1997). Evidence of FCC Crystallization of SiO2 Nanospheres. *Langmuir,* Vol.13, No.23, (November 1997), pp. 6009-6011

Mihi, A., Zhang, C. & Braun, P. V. (2011). Transfer of Preformed Three-Dimensional Photonic Crystals onto Dye-Sensitized Solar Cells. *Angewandte Chemie International Edition,* Vol.50, No.25, (June 2011), pp. 5712-5715

Moroz, A & Sommers, C. (1999). Photonic Band Gaps of Three-dimensional Face-centred Cubic Lattices. *Journal of Physics: Condensed Matter,* Vol.11, No.4, (February 1999), pp. 997-1008

Norris, D. J. & Vlasov, Y. A. (2001). Chemical Approaches to Three-Dimensional Semiconductor Photonic Crystals. *Advanced Materials,* Vol.13, No. 6, (March 2001), pp. 371-376

Ozin, G. A. & Yang, S. M. (2001). The Race for the Photonic Chip: Colloidal Crystal Assembly in Silicon Wafers. *Advanced Functional Materials,* Vol.11, No.2, (April 2001), pp. 95-104

Park, S. H., Qin, D. & Xia, Y. (1998). Crystallization of Mesoscale Particles over Large Areas. *Advanced Materials,* Vol.10, No.13, (September 1998), pp. 1028-1032

Park, S. H., Gates, B. & Xia, Y. (1999). A Three-Dimensional Photonic Crystal Operating in the Visible Region. *Advanced Materials,* Vol.11, No.6, (April 1999), pp. 462-466

Pieranski, P. (1983). Colloidal Crystals. *Contemporary Physics*, Vol.24, No.1, (January 1983), pp. 25-73, ISSN 00107514

Pradhan, R. D., Bloodgood, J. A. & Watson, G. H. (1997). Photonic Band Structure of bcc Colloidal Crystals. *Physical Review B,* Vol.55, No.15, (April 1997), pp. 9503-9507

Prieve, D. C., Sides, P. J. & Wirth, C. L. (2010). 2-D Assembly of Colloidal Particles on a Planar Electrode. *Current Opinion in Colloid & Interface Science,* Vol.15, No.3, (June 2010), pp. 160-174

Pusey, P. N. & van Megen, W. (1986). Phase Behaviour of Concentrated Suspensions of Nearly Hard Colloidal Spheres. *Nature,* Vol.320, No.6060, (March 1986), pp. 340-342.

Pusey, P. N., van Megen, W., Bartlett, P., Ackerson, B. J., Rarity, J. G. & Underwood, S. M. (1989). Structure of Crystals of Hard Colloidal Spheres. *Physical Review Letters,* Vol.63, No.25, (December 1989), pp. 2753-2756

Rai-Choudhury, P. (1997). *Handbook of Microlithography, Micromachining, and Microfabrication: Microlithography*, SPIE Press, ISBN 9780819423788

Ray, M. A., Kim, H. & Jia, L. Dynamic Self-Assembly of Polymer Colloids to Form Linear Patterns. *Langmuir,* Vol.21, No.11, (May 2005), pp. 4786-4789

Ramiro-Manzano, F., Bonet, E., Rodriguez, I. & Meseguer, F. (2009). Layering Transitions in Colloidal Crystal Thin Films between 1 and 4 Monolayers. *Soft Matter,* Vol.5, No.21, (2009), pp. 4279-4282

Romano, F. & Sciortino, F. (2011). Colloidal Self-assembly: Patchy from the Bottom Up. *Nat Mater,* Vol.10, No.3, (March 2011), pp. 171-173

Sasaki, M. & Hane, K. (1996). Ultrasonically Facilitated Two-dimensional Crystallization of Colloid Particles. *Journal of Applied Physics,* Vol.80, No.9, (1996), pp. 5427-5431

Schmidt, M. & Löwen, H. (1997). Phase Diagram of Hard Spheres Confined between Two Parallel Plates. *Physical Review E,* Vol.55, No.6, (June 1997), pp. 7228-7241

Sharma, A. & Reiter, G. (1996). Instability of Thin Polymer Films on Coated Substrates: Rupture, Dewetting, and Drop Formation. *Journal of Colloid and Interface Science,* Vol.178, No.2, (March 1996), pp. 383-399

Sharma, V., Yan, Q., Wong, C. C., Carter, W. C. & Chiang, Y. M. (2009). Controlled and Rapid Ordering of Oppositely Charged Colloidal Particles. *Journal of Colloid and Interface Science,* Vol.333, No.1, (May 2009), pp. 230-236

Sirota, E. B., Ou-Yang, H. D., Sinha, S. K., Chaikin, P. M., Axe, J. D. & Fujii, Y. (1989). Complete Phase Diagram of a Charged Colloidal System: A Synchro-tron X-ray Scattering Study. *Physical Review Letters*, Vol.62, No.13, (March 1989), pp. 1524-1527

Tan, K. W., Li, G., Koh, Y.K., Yan, Q. & Wong, C. C. (2008). Layer-by-Layer Growth of Attractive Binary Colloidal Particles. *Langmuir,* Vol.24, No.17, (July 2008), pp. 9273-9278

Tan, K. W., Koh, Y. K., Chiang, Y.M. & Wong, C. C. (2010). Particulate Mobility in Vertical Deposition of Attractive Monolayer Colloidal Crystals. *Langmuir*, Vol.26, No.10 (May 2010), pp. 7093-7100.

Teh, L. K., Tan, N. K., Wong, C. C. & Li, S. Growth imperfections in three-dimensional colloidal self-assembly. *Applied Physics A: Materials Science & Processing*, Vol. 81, No. 7, (November 2005), pp. 1399-1404

Thijssen, J. H. J., Petukhov, A. V., 't Hart, T. C., Imhof, A., van der Werf, C. H. M., Schropp, R. E. I. & van Blaaderen, A. (2006). Characterization of Photonic Colloidal Single Crystals by Microradian X-ray Diffraction. *Advanced Materials,* Vol.18, No.13, (July 2006), pp. 1662-1666

Thomson, N. R., Bower, C. L. & McComb, D. W. (2008). Identification of Mechanisms Competing with Self-assembly during Directed Colloidal Deposition. *Journal of Materials Chemistry.* Vol.18, No.21, (2008), pp. 2500-2505

Tien, J., Terfort, A. & Whitesides, G. M. (1997). Microfabrication through Electrostatic Self-Assembly. *Langmuir,* Vol.13, No.20, (October 1997), pp. 5349-5355

Torres, C. M. S. (2003) *Alternative lithography: unleashing the potentials of nanotechnology,* Springer, ISBN 9780306478581

Troian, S. M., Herbolzheimer, E., Safran, S. A. & Joanny, J. F. (1989). Fingering Instabilities of Driven Spreading Films. *Europhysics Letters (EPL),* Vol.10, No.1, (September 1989), pp. 25-30

Ulman, A. (1996). Formation and Structure of Self-Assembled Monolayers. *Chemical Reviews,* Vol.96, No.4, (January 1996), pp. 1533-1554

van Blaaderen, A., Ruel, R. & Wiltzius, P. (1997). Template-directed Colloidal Crystallization. *Nature,* Vol.385, No.6614, (January 1997), pp. 321-324

van Rijn, C. J. M., Veldhuis, G. J. & Kuiper, S. (1998). Nanosieves with Microsystem Technology for Microfiltration Applications. *Nanotechnology,* Vol.9, No.4, (December 1998), pp. 343-345

Velev, O. D. & Lenhoff, A. M. (2000). Colloidal Crystals as Templates for Porous Materials. *Current Opinion in Colloid & Interface Science,* Vol.5, No.1-2, (March 2000), pp. 56-63

Vlasov, Y. A., Astratov, V. N., Baryshev, A. V., Kaplyanskii, A. A., Karimov, O. Z. & Limonov, A. F. (2000). Manifestation of Intrinsic Defects in Optical Properties of Self-organized Opal Photonic Crystals. *Physical Review E,* Vol.61, No.5, (May 2000), pp. 5784-5793

Vos, W. L., Sprik, R., van Blaaderen, A., Imhof, A., Lagendijk, A. & Wegdam, G. H. (1996). Strong Effects of Photonic Band Structures on the Diffraction of Colloidal Crystals. *Physical Review B,* Vol.53, No.24, (June 1996), pp. 16231-16235

Vos, W. L., Megens, M., van Kats, C. M. & Bösecke, P. (1997). X-ray Diffraction of Photonic Colloidal Single Crystals. *Langmuir,* Vol.13, No.23, (November 1997), pp. 6004-6008

Williams, R. & Crandall, R. S. (1974). The Structure of Crystallized Suspensions of Polystyrene Spheres. *Physics Letters A,* Vol.48, No.3, (June 1974), pp. 225-226

Xia, Y & Whitesides, G. M. (1998). Soft Lithography. *Angewandte Chemie International Edition,* Vol.37, No.5, (March 1998), pp. 550-575

Yablonovitch, E. (1987). Inhibited Spontaneous Emission in Solid-State Physics and Electronics. *Physical Review Letters,* Vol.58, No.20, (May 1987), pp. 2059-2062

Yan, Q., Gao, L., Sharma, V., Chiang, Y.M. & Wong, C. C. (2008). Particle and Substrate Charge Effects on Colloidal Self-Assembly in a Sessile Drop. *Langmuir,* Vol. 24, No.20, (October 2008), pp. 11518-11522

Yan, Q., Pavan, N., Chiang, Y. M. & Wong, C. C. (2009). Three-dimensional Metallic Opals Fabricated by Double Templating. *Thin Solid Films,* Vol.517, No.17, (July 2009), pp. 5166-5171

Yang, S. M. & Ozin, G. A. (2000). Opal Chips: Vectorial Growth of Colloidal Crystal Patterns inside Silicon Wafers. *Chemical Communications*, No.24, (2000), pp. 2507-2508

Yethiraj, A. & van Blaaderen, A. (2003). A Colloidal Model System with an Interaction Tunable from Hard Sphere to Soft and Dipolar. *Nature,* Vol.421, No.6922, (January 2003), pp. 513-517

Yethiraj, A., Wouterse, A., Groh, B. & van Blaaderen, A. (2004), Nature of an Electric-Field-Induced Colloidal Martensitic Transition. *Physical Review Letters,* Vol.92, No.5, (February 2004), pp. 058301-1 – 058301-4

Yoshiyama, T., Sogami, I. & Ise, N. (1984). Kossel Line Analysis on Colloidal Crystals in Semidilute Aqueous Solutions. *Physical Review Letters,* Vol.53, No.22, (November 1984), pp. 2153-2158

Zhang, K. & Liu, X. Y. (2004). In Situ Observation of Colloidal Monolayer Nucleation Driven by an Alternating Electric Field. *Nature,* Vol.429, No.6993, (June 2004), pp. 739-743

Zhou, Z. & Zhao, X. S. (2004). Flow-Controlled Vertical Deposition Method for the Fabrication of Photonic Crystals. *Langmuir* Vol.20, No.4, (February 2004), pp. 1524-1526

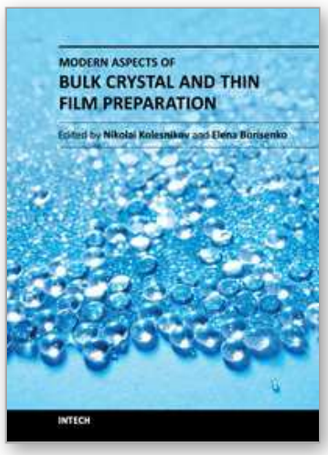

Modern Aspects of Bulk Crystal and Thin Film Preparation

Edited by Dr. Nikolai Kolesnikov

ISBN 978-953-307-610-2
Hard cover, 608 pages
Publisher InTech
Published online 13, January, 2012
Published in print edition January, 2012

In modern research and development, materials manufacturing crystal growth is known as a way to solve a wide range of technological tasks in the fabrication of materials with preset properties. This book allows a reader to gain insight into selected aspects of the field, including growth of bulk inorganic crystals, preparation of thin films, low-dimensional structures, crystallization of proteins, and other organic compounds.

How to reference

In order to correctly reference this scholarly work, feel free to copy and paste the following:

E. C. H. Ng, Y. K. Koh and C. C. Wong (2012). Colloidal Crystals, Modern Aspects of Bulk Crystal and Thin Film Preparation, Dr. Nikolai Kolesnikov (Ed.), ISBN: 978-953-307-610-2, InTech, Available from: http://www.intechopen.com/books/modern-aspects-of-bulk-crystal-and-thin-film-preparation/colloidal-crystals

INTECH
open science | open minds

InTech Europe
University Campus STeP Ri
Slavka Krautzeka 83/A
51000 Rijeka, Croatia
Phone: +385 (51) 770 447
Fax: +385 (51) 686 166
www.intechopen.com

InTech China
Unit 405, Office Block, Hotel Equatorial Shanghai
No.65, Yan An Road (West), Shanghai, 200040, China
中国上海市延安西路65号上海国际贵都大饭店办公楼405单元
Phone: +86-21-62489820
Fax: +86-21-62489821

IntechOpen